AIP | Journal of Applied Physics

Color stable white phosphorescent organic light emitting diodes with red emissive electron transport layer

Jin Wook Kim, Seung Il Yoo, Jin Sung Kang, Song Eun Lee, Young Kwan Kim, Hyeong Hwa Yu, Ayse Turak, and Woo Young Kim

Citation: Journal of Applied Physics **117**, 245503 (2015); doi: 10.1063/1.4923048
View online: http://dx.doi.org/10.1063/1.4923048
View Table of Contents: http://scitation.aip.org/content/aip/journal/jap/117/24?ver=pdfcov
Published by the AIP Publishing

Color stable white phosphorescent organic light emitting diodes with red emissive electron transport layer

Jin Wook Kim,[1] Seung Il Yoo,[1] Jin Sung Kang,[1] Song Eun Lee,[2] Young Kwan Kim,[2] Hyeong Hwa Yu,[3] Ayse Turak,[3] and Woo Young Kim[1,3,a)]
[1]*Department of Green Energy & Semiconductor Engineering, Hoseo University, Asan 336-795, South Korea*
[2]*Department of Information Display, Hongik University, Seoul 121-791, South Korea*
[3]*Department of Engineering Physics, McMaster University, Hamilton, Ontario L8S 4L7, Canada*

(Received 6 March 2015; accepted 16 June 2015; published online 30 June 2015)

We analyzed the performance of multi-emissive white phosphorescent organic light-emitting diodes (PHOLEDs) in relation to various red emitting sites of hole and electron transport layers (HTL and ETL). The shift of the recombination zone producing stable white emission in PHOLEDs was utilized as luminance was increased with red emission in its electron transport layer. Multi-emissive white PHOLEDs including the red light emitting electron transport layer yielded maximum external quantum efficiency of 17.4% with CIE color coordinates (−0.030, +0.001) shifting only from 1000 to 10 000 cd/m^2. Additionally, we observed a reduction of energy loss in the white PHOLED via Ir(piq)$_3$ as phosphorescent red dopant in electron transport layer. [http://dx.doi.org/10.1063/1.4923048]

I. INTRODUCTION

White phosphorescent organic light emitting diodes (PHOLEDs) have gained tremendous attention due to their significant potential application in solid state lighting and flat panel or flexible displays.[1–6] Applying this technology may require white PHOLEDs to achieve high external quantum efficiency (EQE), high color rendering index (CRI), proper CIE$_{XY}$ color coordinates, and high color stability. In order to meet these requirements, different device designs and optimization are desired for high performance in commercial applications.[7–11] For color stable white emission, it is essential to control a combination of three primary colors or at least two complimentary colors via concentration and/or position adjustment in the emissive layer. Two color and three color (blue, green, and red) white in single and multi-emissive layers have formally been used to produce white PHOLEDs.[12–16] Single emissive white PHOLEDs, compared to multi-emissive white PHOLEDs, go through an additional exciton energy transfer process. When two or three phosphorescent dopants are close to each other, energy transfer occurs from a higher energy level to a lower energy level via Foster and Dexter energy transfer mechanisms. Therefore, usually the red dopant with a lower triplet energy level is saturated first, followed by green and blue dopants consecutively.[17] Eventually, this increases the driving voltage, leading to lower color stability on white PHOLEDs due to insufficient red emission.[16,18–23] In multi-emissive white PHOLEDs, the color emissive site has a higher possibility of color stability. However, the shift of the recombination zone causes problems for stable white emission in the multi-emissive layer. The charge carrier recombination zone is usually formed near the interface between the emissive layer and the hole/electron transport layer.[24,25] Then, the recombination zone shifts as the driving voltage increases, resulting in poor color stability for multi-emissive white PHOLEDs. Typically, hole and electron recombination are confined in the emissive layer by device engineering through the methods, such as optimization of hole and electron transport layer thickness, and introduction to hole and electron blocking layer. However, shifts of the recombination zone into the hole and electron transport layers have been shown to improve the device performance.[26,27]

In this study, highly colour-stabled white PHOLEDs with a multi-emissive layer were observed. We took advantage of the generally problematic shift of the recombination zone with increasing in driving voltage to achieve stable white emission by doping the transport layer with a red emitter multi-emissive white PHOLEDs. The location of the recombination zone and the reduction of charge carrier loss due to red light emission was confirmed by varying the thickness of the hole and electron transport layer doped with 3% of Ir(piq)$_3$ as red dopant (thickness x and y). The extension of the recombination zone into the hole and electron transport layer by doping with Ir(piq)$_3$ greatly enhanced both the EQE and stable white emission.

II. EXPERIMENT

White PHOLEDs were fabricated in device architecture: ITO (150 nm)/NPB (70-x nm)/NPB:Ir(piq)$_3$–3% (x nm)/mCP:Ir(ppy)$_3$–1%:Ir(piq)$_3$-z%(18 nm)/mCP:FIrpic-8% (12 nm)/TPBi:Ir(piq)$_3$–3% (y nm)/TPBi (30-y nm)/Liq (2 nm)/Al (120 nm). Indium tin oxide (ITO) coated glasses with a sheet resistance of ∼12 Ω/sq were used for the substrate. Line patterns of ITO were formed using a photolithography process. The ITO glass substrates were cleaned in an ultrasonic bath in sequence with deionized water, isopropyl alcohol, acetone, deionized water, and isopropyl alcohol. The ITO/glass substrates were then treated with O_2 plasma under vacuum conditions of 5.0×10^{-2} Torr and of 50 W for 2 min. All

a)Author to whom correspondence should be addressed. Electronic mail: wykim@hoseo.edu

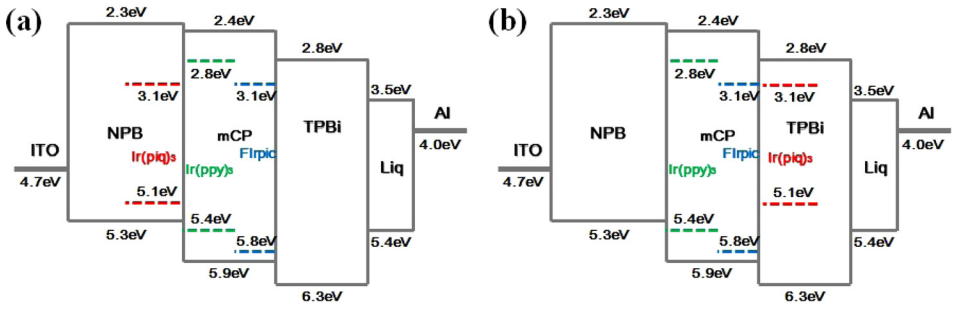

FIG. 1. Schematic energy band diagrams of white PHOLEDs. $Ir(piq)_3$ doped into (a) hole transport layer (NPB) and (b) electron transport layer (TPBi).

organic materials were deposited by thermal evaporation at a pressure of $\sim 1.0 \times 10^{-7}$ Torr. Hole transport materials of N,N′-diphenyl-N,N′-bis(l-naphthyl-phenyl)–(l,l′-biphenyl)–4,4′–diamine (NPB), a host material of N,N′-dicarbazolyl-3,5-benzene (mCP), blue, green, and red phosphorescent dopants of Bis(3,5-difluoro-2 -(2-pyridyl)-phenyl-(2-carboxypyridyl) iridium(III) (FIrpic), Tris(2-phenylpyridine)iridium(III) ($Ir(ppy)_3$), and Tris(1-phenylisoquinoline)iridium(III) ($Ir(piq)_3$), an electron transport layer of 2′,2′,2″-(1,3,5-Benzinetriyl)-tris(1-phenyl-1-H-benzimidazole) (TPBi), and an electron injection layer of 8-Hydroxyquinolinolato-lithium (Liq) were used for white PHOLED device fabrication. The aluminum cathode was formed by thermal evaporation at an evaporation rate of 5.0 Å/s. All fabricated devices have the active area of $3 \times 3\,mm^2$, as defined by the shadow mask used for cathode deposition. The electro-optical characteristics of the white PHOLEDs were measured and analyzed using a Keithley 238 LMS PR-650 spectrophotometer, colorimeter, and the current density-voltage-luminance (J-V-L) system. Photo absorption and photoluminescence (PL) spectra of hole and electron transport molecules and dopant molecules were measured in CH_2Cl_2 at room temperature. Fig. 1 shows schematic energy band diagrams of white PHOLED devices A and B and the corresponding energy levels of the highest occupied and lowest unoccupied molecular orbitals (HOMO/LUMO).[21,28–33]

III. RESULTS AND DISCUSSION

As shown in Table I, we fabricated devices A1, A2, A3, A4, and reference in order of ITO (150 nm)/NPB (70-x nm)/NPB:$Ir(piq)_3$–3% (x nm)/mCP:$Ir(ppy)_3$–1% (18 nm)/mCP:FIrpic-8% (12 nm)/TPBi:$Ir(piq)_3$–3% (y nm)/TPBi (30-y nm)/Liq (2 nm)/Al (120 nm), where x = 2.5, 10, 0, 0, and 0 and y = 0, 0, 2.5, 10, and 0 to tailor the recombination zone position by observing the electroluminescence (EL) spectral behaviors resulting from modifications of the recombination zone position. The doping concentration of FIrpic and $Ir(ppy)_3$ and thickness of emissive layer in the reference device, which has no red emission from $Ir(piq)_3$, was optimized by previous experiments to achieve better performance according to triplet-triplet energy transfer from host to dopants. In case of blue dopant concentration, we designed the reference device to have higher external quantum efficiency, such as mCP:FIrpic-8% of emissive layer (more than 8% of FIrpic had been quenched), whereas mCP:$Ir(ppy)_3$–1% of emissive layer used as supplementing insufficient green emission. Then, we realized that the emissive layer, which is mCP:$Ir(ppy)_3$–1% (18 nm)/mCP:FIrpic-8% (12 nm), has best performance for this reference structure.

TABLE I. Summary of different red light emitting site used in the multi-emissive layer of white PHOLEDs of the type: ITO (150 nm)/NPB (70-x nm)/NPB:$Ir(piq)_3$-3% (x nm)/mCP:$Ir(ppy)_3$-1% (18 nm)/mCP:FIrpic-8% (12 nm)/TPBi:$Ir(piq)_3$-3% (y nm)/TPBi (30-y nm)/Liq (2 nm)/Al (120 nm).

Device	x	y
A1	2.5	0
A2	10	0
A3	0	2.5
A4	0	10
Reference	0	0

As described in Fig. 2, the photoluminescence spectra of NPB and TPBi as hole and electron transport materials overlaps well with the absorption bands of $Ir(piq)_3$, implying a high rate of Forster energy transfer from NPB and TPBi to $Ir(piq)_3$. The rate constant k_{ET} of Foster energy transfer mechanism can be expressed by following two equations:

$$k_{ET} = \left\{\frac{1}{\tau_s}\right\}\left(\frac{R_0}{\mathrm{r}}\right)^6$$

and

$$R_0{}^6 = \frac{9000(ln10)\kappa^2\Phi_F}{128\pi^5 N n^4}\int_0^{\lambda} F(\lambda)\varepsilon(\lambda)\lambda^4 d\lambda\,,$$

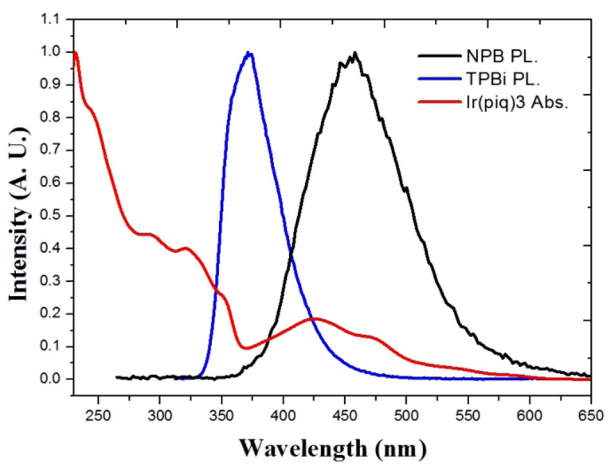

FIG. 2. PL measured for NPB and TPBi and the absorption spectra of $Ir(piq)_3$.

where τ_s is the life time, R_0 is the Foster radius, r is the distance between donor and acceptor, κ^2 is the orientation factor, Φ_F is the photoluminescence quantum efficiency, N is the Avogadro's number, n is the refractive index, $\int_0^{\lambda} F(\lambda)\varepsilon(\lambda)\lambda^4 d\lambda$ is the spectral overlap integral between donor photoluminescence $(F(\lambda))$, $\varepsilon(\lambda)$ is the acceptor absorption, and λ is the wavelength. From the rate constant k_{ET} of Foster energy transfer mechanism, one would expect more energy transfer for NPB than for TPBi, as the spectral overlap of the PL and $Ir(piq)_3$ absorbance is much larger (assuming it is proportional to the efficiency).

Fig. 3 shows normalized EL spectra of devices A1, A2, A3, and A4 from luminance 1000 to 10 000 cd/m^2. As shown in Fig. 3, emission peak around 470 nm, 500 nm, and 615 nm are FIrpic, $Ir(ppy)_3$, and $Ir(piq)_3$ emission peak as blue, green, and red, respectively. Doping of $Ir(piq)_3$ into the hole transport layer (HTL) near the emission zone (A1 and A2) has a slight impact on the EL characteristics of the reference device, with very little emission from the $Ir(piq)_3$. This suggests that there is very little energy transfer from the NPB layer, despite good spectral overlap. Doping into the electron transport layer (ETL), on the other hand, had significant impact on the EL intensity, with strong emission from the $Ir(piq)_3$, confirming that the main recombination zone is positioned at the interface between the emissive layer and electron transport layers. By the way, as shown in Figs. 3(c) and 3(d), there is stronger intensity of blue emission than that of red emission although recombination zone is positioned at the interface between blue and red emission zone. The reason for this phenomenon is caused by higher blue doping concentration generating more triplet-triplet energy transfer according to exponential reduction with distance between the host and dopant. Therefore, relatively lower doping concentration of red dopant has lower probability of triplet-triplet energy transfer from host to dopant. Fig. 4 shows both the evolution of recombination zone position with layer thickness and spectra changes with doping. There are similar characteristics between EL spectra of devices A3 and A4. But, emission peak intensity of the A4 has slightly higher than that of the A3 around 615 nm due to difference of parameter r, which is the distance between donor and acceptor. Even though the recombination zone occur at the interface between ETL/emission zone, the device A4, which has thicker red doping zone, has efficient Foster energy transfer because of ~10 nm of its radius. This result demonstrate that charge recombination zone occur almost within 2.5 nm from the interface between ETL/emission zone but remaining energy can be transferred out of radius 2.5 nm. Both A3 and A4 show decreasing emission at 615 nm as luminance increases from 1000 to 10 000 cd/m^2 indicating that the recombination zone shifts into the emissive layer under applied bias. Additionally, there are relatively different emission intensities from 400 nm to 450 nm between the spectra of one group (devices A1 and A2) and that of the

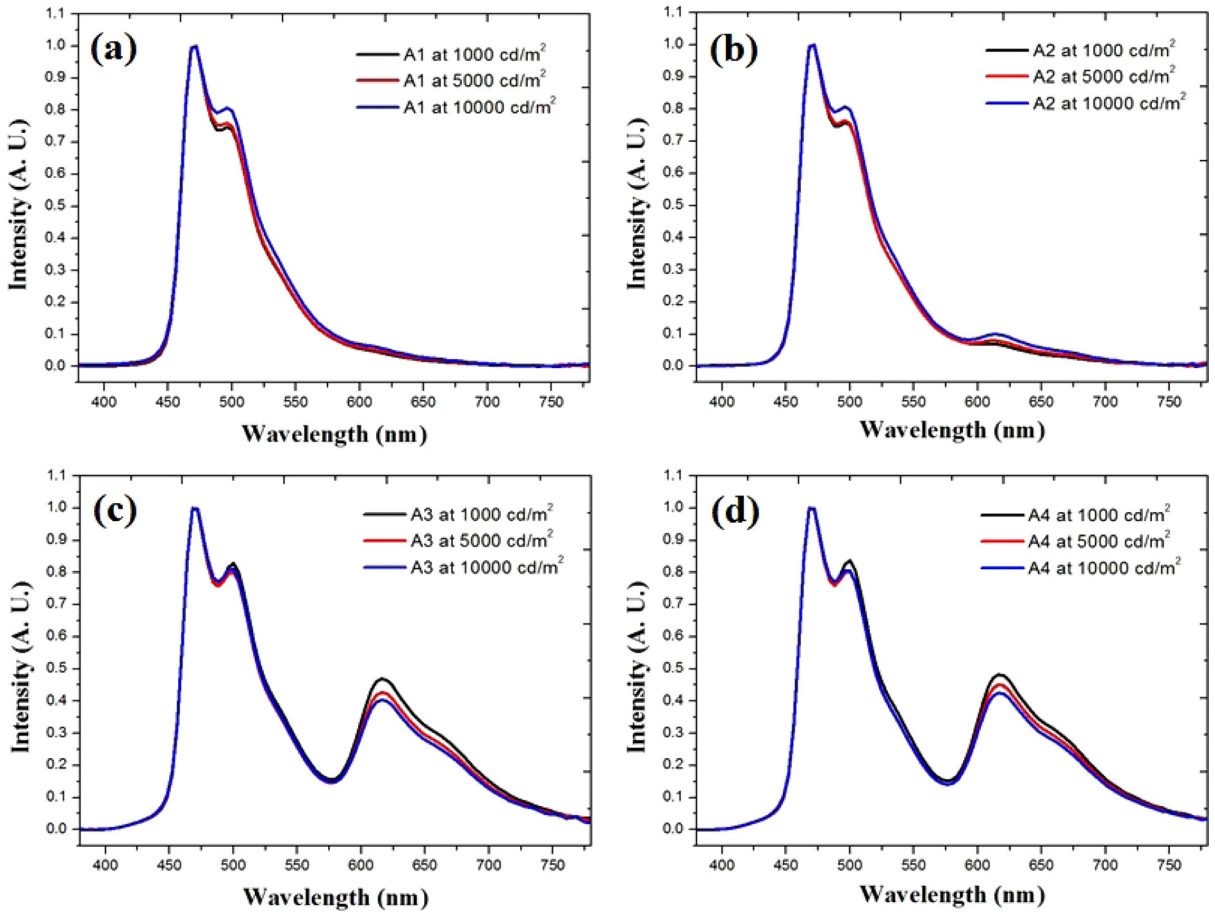

FIG. 3. EL spectra of white PHOLEDs A1, A2, A3, and A4 as luminance increases from 1000 to 10 000 cd/m^2.

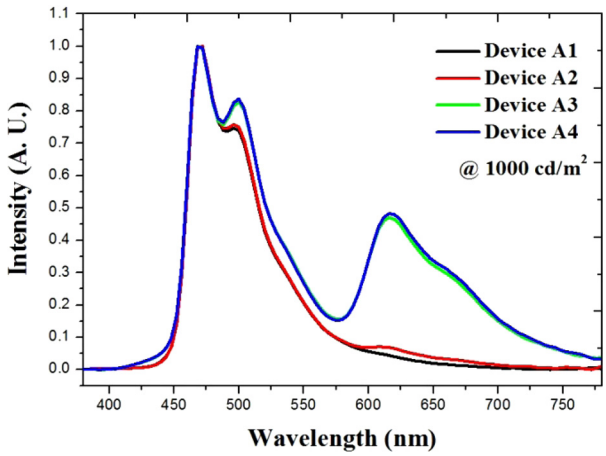

FIG. 4. Compare to EL spectra of white PHOLEDs A1, A2, A3, and A4 at 1000 cd/m^2.

other group (devices A3 and A4). This phenomenon can be explained in terms of NPB's emission as hole transport layer due to existence of leakage current in NPB. As shown in Fig. 4, main peak intensity is contributed to peak difference, appeared around 450 nm. EL peak at 450 nm matches well with PL emission spectrum of NPB (see Fig. 2), whereas in case of the devices A1 and A2, the reason for no emission peak intensity between 400 nm and 450 nm is due to emission of Ir(piq)$_3$ as red dopant overwhelmed NPB emission intensity. Although there appears to be no significant Forster energy transfer from NPB, there is a small but visible feature at 615 nm, which is unchanged in A1 but increases in A2 with increasing luminance (see Fig. 3). This is likely due to direct recombination on the dopant resulting from charge trapping[17,34–36] from the 0.2 eV offset of the HOMO energies between NPB and Ir(piq)$_3$. Thus, due to the thicker red doping zone, A2 has a higher red peak around 615 nm than A1.

Fig. 5 shows current density and luminance-voltage and EQE-current density characteristics of devices A1, A2, A3, A4, and reference. The similarity in the device performance for the ETL doped samples (A3, A4) with the reference device suggests that the recombination zone position is likely originally at the ETL/emission zone interface. Devices A1 and A2 have lower current density than the other devices, most likely due to the loss of holes from charge trapping, supporting the previously proposed mechanism for red emission. While the ETL doped and reference samples had undoped HTL layers, allowing undisturbed conduction of holes, A1 and A2 had some transfer of energy to the Ir(piq)$_3$ molecules, disturbing the charge flow, and lowering the current density, as the mobility of holes is one to two orders of magnitude higher than that of electrons in these devices. The hole carrier had been arrived first at either interface between emissive layer and electron transfer layer or inside of electron transfer layer before the electron carrier could be arrived

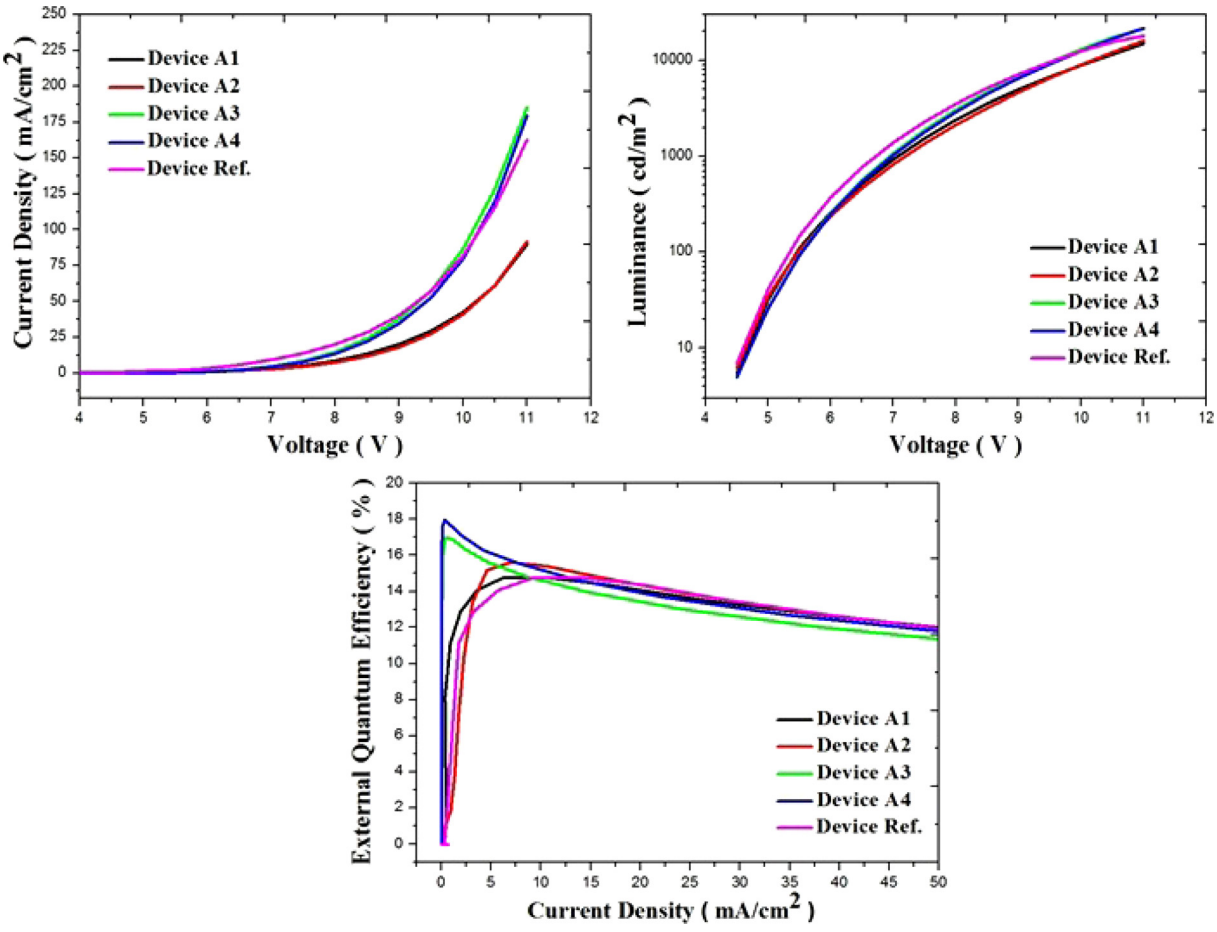

FIG. 5. Current density and luminance characteristics as driving voltage increased and EQE-current density characteristics of devices A1, A2, A3, A4, and reference.

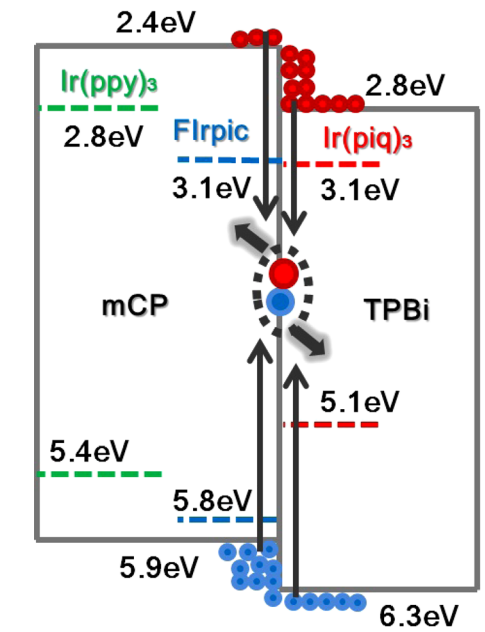

FIG. 6. Formation of recombination zone at both interfaces between emissive layer and electron transfer layer, and inside of electron transfer layer.

at the interface. This is the reason that current density properties could not be almost affected by electron carrier.

The properties of EQE show that devices A3 and A4 have higher EQE than those of other devices at initial current density ($\sim$10 mA/cm^2) due to preventing energy loss caused utilization of red dopant in electron transport layer. Thereafter, an increase in current density, the EQE curve of devices A1, A2, A3, A4, and reference shows identical EQE curve characteristics. This phenomenon suggests shift of recombination zone to inside of emissive layer (mCP:FIrpic-8%) as current density increases. This also supports the proposed location of the recombination zone positioned at the interface between emissive layer and electron transport layer. Usually, charge carriers are accumulated in the interface between different organic materials as a result of the difference in energy barriers. As shown in Fig. 6, by utilizing some of the accumulated charges in the ETL for red emission with the Ir(piq)$_3$ dopant, the external quantum efficiency of the device can increase.

After establishing that the emission zone is located at the ETL interface, and that using the ETL for red emission by doping leads to higher EQE, a second set of devices, B1, B2, and B3 were fabricated to supplement the insufficient red emission from device A3 for stable white emission. In this set of devices, the Ir(piq)$_3$ was directly doped into the emission layer (mCP) close to the HTL side of the device, along with the green dopant Ir(ppy)$_3$, in the device: ITO (150 nm)/NPB (70 nm)/mCP:Ir(ppy)$_3$–1%:Ir(piq)$_3$-z% (18 nm)/mCP:FIrpic-8% (12 nm)/TPBi:Ir(piq)$_3$–3% (2.5 nm)/TPBi (27.5 nm)/Liq (2 nm)/Al (120 nm), where z = 1, 2, and 3.

As seen in Fig. 7, increasing the red dopant in the mCP layer decreases the CIEx value significantly, while the CIEy values increased slightly (see Table II), hence, B1 has the most stable white, nearest to 0.32, 0.33. Additionally, the CIE$_Y$ of devices B1, B2, and B3 increased as luminance increased from 1000 to 10 000 cd/m^2. These results can be explained using a triplet-triplet energy transfer mechanism.[37] When Ir(ppy)$_3$ and Ir(piq)$_3$ are close to each other, within the probable radius of triplet-triplet energy transfer, the triplet excitons seem to move from the higher triplet energy level of Ir(ppy)$_3$ to the lower triplet energy level of Ir(piq)$_3$ until the red dopants are fully excited by triplet excitons. After that the Ir(ppy)$_3$ contributes to green emission. According to early mentioned triplet-triplet energy transfer mechanism, green dopant Ir(ppy)$_3$ contributes to form hole injection barrier and inhibits hole injection until 5000 cd/m^2 in the device B1 as well as A3 and A4 but Ir(ppy)$_3$ can also contribute to generate green emission after 5000 cd/m^2. In other words, Ir(piq)$_3$ starts to emit, whereas Ir(ppy)$_3$ only take a role to be hole injection barrier until 5000 cd/m^2. This result can be implied that CIE$_Y$ coordinates of the device B1 became lower at 5000 cd/m^2 and then it did higher as brightness was increased to 10 000 cd/m^2, as shown in Fig. 7.

Fig. 8 shows predicted white CIE$_{XY}$ color coordinates of calculated white emission based upon photoluminescence of FIrpic, Ir(ppy)$_3$, and Ir(piq)$_3$ peak wave-length is about (0.33, 0.33). To obtain perfect white emission, we need to assume energy transfer from donor to acceptor in emission layer and also control ratio of blue, green, and red emission which is dependent on their peak position. As shown in

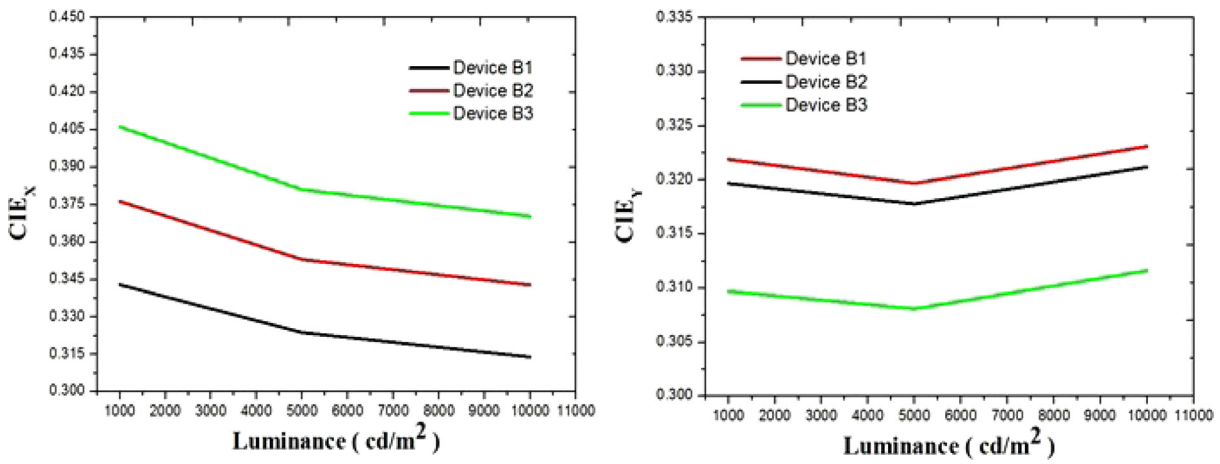

FIG. 7. CIE$_{XY}$-voltage characteristics of devices B1, B2, and B3 as increase in luminance from 1000 to 10 000 cd/m^2.

TABLE II. Maximum EQE and color coordinates of white PHOLED devices B1, B2, and B3.

Device	EQE (%)	Color coordinates	
		ΔCIE_{XY}[a]	CIE_{XY}[b]
B1	17.4	(−0.030, 0.001)	(0.343, 0.322)
B2	17.2	(−0.034, 0.002)	(0.376, 0.320)
B3	16.5	(−0.036, 0.002)	(0.406, 0.310)

[a]CIE_{XY} difference at 1000 cd/m^2 and 10 000 cd/m^2.
[b]CIE_{XY} at 1000 cd/m^2.

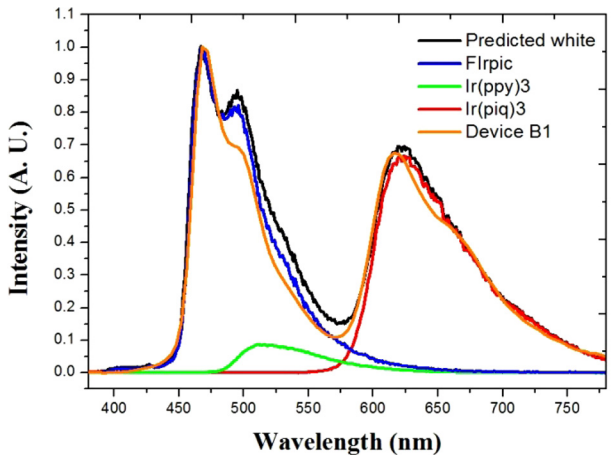

FIG. 8. Predicted white emission spectrum which is CIE_{XY} color coordinates (0.33, 0.33) combining the photoluminescence of blue, green, and red each dopant and the device B1 emission spectrum.

Fig. 8, the device B1 spectrum is similar to the predicted white emission spectrum.[38]

Table II shows maximum EQE and color coordinates of white PHOLED devices B1, B2, and B3. Considering appropriate white light emission with color stability and EQE, device B1 shows reasonable CIE_{XY} color coordinates of (0.343, 0.322) at 1000 cd/m^2, which are closer to ideal white CIE_{XY} color coordinates of (0.33, 0.33) and higher EQE 17.4% than the devices B2 and B3.

IV. CONCLUSION

This study investigated the performance of multi-emissive layer white PHOLEDs fabricated with red light emitting of electron transport layer. The results show that the formation of the recombination zone in the interface between emissive layer and electron transport layer affects the EQE and white color stability in white PHOLED devices. Additionally, extending the recombination zone into the transport layer is favorable for efficient performance in multi-emissive layer PHOLEDs, due to the reduction of energy loss in the interface between emissive layer and transport layer where energy barriers normally exist. We were able to produce optimized multi-emissive layer white PHOLEDs with 17.4% EQE and slight changes in CIE_{XY} color coordinates (−0.030, 0.001), by doping the electron transport layer with a red dopant. We will continue additional experiments for next paper using other host materials such as CDBP possessing a higher triplet energy level of 2.9 eV and better thermal stability to achieve better performances.

[1]B. W. D'Andrade and S. R. Forrest, Adv. Mater. **16**, 1585–1595 (2004).
[2]P. E. Burrows *et al.*, IEEE Trans. Electron Devices **44**, 1188–1203 (1997).
[3]R. F. Service, Science **310**, 1762–1763 (2005).
[4]J. Kido, M. Kimura, and K. Nagai, Science **44**, 1188 (1995).
[5]G. He, M. Pfeiffer, K. Leo, M. Hofmann, J. Birnstock, R. Pudzich, and J. Salbeck, Appl. Phys. Lett. **85**, 3911 (2004).
[6]M. A. Baldo, M. E. Thompson, and S. R. Forrest, Nature **403**, 750 (2000).
[7]M. A. Baldo *et al.*, Appl. Phys. Lett. **75**, 4–6 (1999).
[8]C. Adachi, M. A. Baldo, S. R. Forrest, and M. E. Thompson, Appl. Phys. Lett. **77**, 904–906 (2000).
[9]C. Adachi, M. A. Baldo, M. E. Thompson, and S. R. Forrest, Appl. Phys. Lett. **90**, 5048–5051 (2001).
[10]C. Adachi *et al.*, Appl. Phys. Lett. **78**, 1622–1624 (2001).
[11]C. Adachi *et al.*, Appl. Phys. Lett. **79**, 2082–2084 (2001).
[12]W. H. Choi, H. L. Tam, F. R. Zhu, D. G. Ma, H. Sasabe, and J. Kido, Appl. Phys. Lett. **102**, 153308 (2013).
[13]C. Weichsel, S. Reineke, M. Furno, B. Lussem, and K. Leo, Appl. Phys. Lett. **111**, 0102 (2012).
[14]U. S. Bhansali, H. Jia, M. A. Q. Lopez, B. E. Gnade, W.-H. Chen, and M. A. Omary, Appl. Phys. Lett. **94**, 203501 (2009).
[15]J. H. Seo, I. H. Park, G. Y. Kim, K. H. Lee, M. K. Kim, S. S. Yoon, and Y. K. Kim, Appl. Phys. Lett. **92**, 183303 (2008).
[16]Y. Sun, N. C. Giebink, H. Kanno, B. Ma, M. E. Tompson, and S. R. Forrest, Nature **440**, 908 (2006).
[17]J. W. Kim, S. I. You, N. H. Kim, J.-A. Yoon, K. W. Cheah, F. R. Zhu, and W. Y. Kim, Sci. Rep. **4**, 7009 (2014).
[18]C. H. Hsiao, Y. H. Lan, P. Y. Lee, T. L. Chiu, and J. H. Lee, Org. Electron. **12**, 547 (2011).
[19]L. C. Meng, Y. B. Hou, Z. D. Lou, F. Teng, X. Yao, X. J. Liu, A. W. Tang, and J. B. Peng, Synth. Met. **172**, 63 (2013).
[20]C. H. Hsiao, S. W. Liu, C. T. Chen, and J. H. Lee, J. Appl. Phys. **106**, 024503 (2009).
[21]W. S. Jeon, T. J. Park, S. Y. Kim, R. Pode, J. Jang, and J. H. Kwon, Org. Electron. **10**, 240 (2009).
[22]L. Hou, L. Duan, J. Qiao, D. Zhang, G. Dong, L. Wang, and Y. Qui, Org. Electron. **11**, 1344 (2010).
[23]Y. S. Tsai, L. A. Hong, F. S. Juang, and C. Y. Chen, J. Lumin. **153**, 312 (2014).
[24]P. Tyagi, R. Srivastava, A. Kumar, S. Tuli, and M. N. Kamalasanan, J. Lumin. **136**, 249–254 (2013).
[25]Z. Ma, S. Zhou, S. Hu, and J. Yu, J. Lumin. **154**, 376–380 (2014).
[26]J. H. Kim, Y. Chen, R. Liu, and F. So, Org. Electron. **15**, 2381–2386 (2014).
[27]P. Zhou, F. Wang, H. Lin, X. Li, L. Tong, N. Wei, Z. Gao, and B. Wei, Solid State Electron. **94**, 6–10 (2014).
[28]J. Jang, J. Ha, and K. Kim, Thin Solid Films **516**, 3152–3156 (2008).
[29]J. A. Yoon, Y. H. Kim, N. H. Kim, C. B. Moon, G. He, and W. Y. Kim, J. Lumin. **153**, 104–108 (2014).
[30]Y. Sun and S. R. Forrest, Appl. Phys. Lett. **91**, 263503 (2007).
[31]C. H. Gao, X. B. Shi, D. Y. Zhou, L. Zhang, Z. K. Wang, and L. S. Liao, Int. J. Photoenergy **2013**, 871765.
[32]X. Wang, J. Zhou, J. Zhao, Z. Lu, and J. Yu, Org. Electron. **21**, 78–85 (2015).
[33]D. Zhao, H. P. Loebl, and V. V. Elsbergen, Org. Electron. **14**, 3117–3122 (2013).
[34]T. C. Liao, H. T. Chou, F. S. Juang, Y. S. Tsai, S. H. Wang, V. Tuan, and Y. Chi, Curr. Appl. Phys. **11**, S175 (2011).
[35]Y. Zhao, L. Zhu, J. Chen, and D. Ma, Org. Electron. **13**, 1340 (2012).
[36]C. B. Moon, W. Song, M. Meng, N. H. Kim, J. A. Yoon, W. Y. Kim, R. Wood, and P. Mascher, J. Lumin. **146**, 314 (2014).
[37]Y. H. Kim, K. W. Cheah, and W. Y. Kim, Appl. Phys. Lett. **103**, 053307 (2013).
[38]N. H. Kim, Y.-H. Kim, J.-A. Yoon, S. Y. Lee, D. H. Ryu, R. Wood, C.-B. Moon, and W. Y. Kim, J. Lumin. **143**, 723–728 (2013).